CONEM 2010 VI Congresso Nacional de Engenharia Mecânica

ABCM COMPROMETIDA COM A PROMOÇÃO DO DESENVOLVIMENTO DA ENGENHARIA E DAS CIÊNCIAS MECÂNICAS
ASSOCIAÇÃO BRASILEIRA DE ENGENHARIA E CIÊNCIAS MECÂNICAS

VI CONGRESSO NACIONAL DE ENGENHARIA MECÂNICA
VI NATIONAL CONGRESS OF MECHANICAL ENGINEERING
18 a 21 de agosto de 2010 – Campina Grande – Paraíba - Brasil
August 18 – 21, 2010 – Campina Grande – Paraíba – Brazil

HYBRID LOAD CALIBRATION OF A STRAIN GAGE INSTRUMENTED HORIZONTAL EMPENNAGE

Jason de Barros, jason.barros@embraer.com.br[1]
João Carlos Menezes, menezes@ita.com.br[2]

[1]Instituto Tecnológico de Aeronática, R. Jales, 324, Bsq. dos Eucaliptos, 12233-680, S. J. dos Campos – SP – Brazil
[2]Instituto Tecnológico de Aeronática, Pç. Mal. Ed. Gomes, 50, V. Acácias, 12228-900, S. J. dos Campos – SP – Brazil

Abstract. *The development of a new transport category airplane or a derivation of an existing airplane with significant changes on its original configuration usually requires a flight test campaign for loads survey. The general purpose of the flight test for loads survey is to validate the theoretical methods used to predict the component loads. The major interest lies in determining the in-flight loads - namely the shear, bending moment and torque - on lifting and stabilizer surfaces, such as wing, horizontal and vertical empennages. Structures instrumented with strain gages and calibrated are commonly used to obtain flight load data. Considering the conventional calibration method, specific loads are applied at various chordwise and spanwise positions over a particular structure surface, and the strain gage responses recorded. From the correlation among loads and strain gage responses, load equations are developed from which surface loads can be determined during the flight test. An alternative load calibration methodology is being proposed using a simplified finite element structural model. In this investigation, a simple NASTRAN structural model of a horizontal empennage was found to be effective in predicting the calibration test strain gage general behavior. The strains prediction represents the basis for this simplified calibration methodology. Provided a suitable adjustment of the model based on some experimental data, the strain gage responses from the actual structure can be satisfactorily predicted by the model. In order to evaluate the alternative calibration methodology reliability, one previously instrumented and (conventionally) calibrated structure was used, providing the reference for both flight and ground test comparisons. The objective of this work is to present the procedures used in adjusting the model responses based on a reduced set of experimental data and to discuss the applicability, advantages and limitations of this methodology.*

Keywords: *In-flight load, Strain Gage, Finite Element Method*

1. INTRODUCTION

The most traditional method used to measure aircraft loads has been through calibrated strain gage installations. This technology emerged in the early 1940's, but only in 1954 it was formalized by Skopinski et al (1954).

In general words, the conventional calibration consists in applying known loads at various spanwise and chordwise positions over a particular strain gage instrumented structure, while recording the strain gage outputs. Then, calibration coefficients are established so the applied loads can be reproduced through the strain gage outputs.

As outlined above, a horizontal empennage of a commercial aircraft was successfully instrumented and calibrated for in-flight loads determination. The results derived from this actual empennage calibration provided the baseline for the present study.

The calibration loading sequence, as applied on the actual structure, was simulated on a simple structural model of the horizontal empennage. As output, the discrete strains at locations corresponding to the strain gages on the actual structure were generated. The discrete strains from the model were mathematically combined into simulated four-active-strain gage bridges, to be consistent with the original strain gage installation.

As expected, discrepancies were found comparing the simulated bridge responses with the experimental ones, since the model does not behaves identically as the actual structure. Then, some adjustments were necessary.

Based on a reduced set of experimental data, it was possible to adjust satisfactorily the model bridge responses. These adjusted bridge responses were used as input to perform a new calibration and a set of load equations were then established. These load equations are intended to reproduce either applied calibration loads or in-flight loads from the experimental bridges responses.

The load equations derived from the new calibration - supported by the structural model - reproduced adequately most of the applied calibration loads, but in general with errors (applied load – calculated load) greater than those verified on the original calibration.

Finally, the in-flight loads were calculated using equations derived from both the conventional calibration and the new one, where a very good correspondence was found.

For this particular structure, it was demonstrated that the load calibration could be performed with the aid of a structural model, provided a suitable strain adjustment based on a reduced set of experimental data.

In this text, the experimental calibration, thoroughly based on physical loading applied to the structure, will be referred as conventional calibration, while the calibration supported by the structural model as hybrid calibration.

2. CONVENTIONAL CALIBRATION

2.1. Instrumentation and Test Setup

The test structure used for this investigation corresponds to the horizontal empennage of one aircraft configured as low-wing and conventional tail. In what follows, it is presented a summary of the calibration test conducted on the prototype.

The horizontal empennage was instrumented with a set of strain gage bridges installed symmetrically in both sides of the empennage root. The load reference points lie on the instrumented stations (one per side).

All strain gages were wired as four-active-arms Wheatstone bridges (full bridges), following the typical arrangement used for bending, shear and torque bridges, as illustrated in Fig. 1. A bending bridge is designed to maximize its response to the bending moment acting on the member where the bridge is installed, while ideally compensated for the other loads. The same concept applies to the shear and torque bridges, respectively for shear load and torque. In common, these bridges are compensated for the uniform thermal deformation on the test material.

The shear and bending bridges were installed on the main spars of the horizontal tail, and the torque bridges on the upper and lower skins.

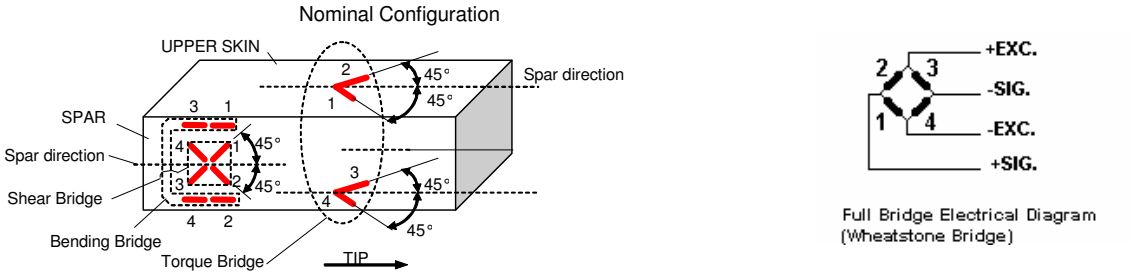

Figure 1: Typical installations for the strain gage bridges

The calibration loads were applied through pads aligned to rib lines, in a total of 4 pads (or load stations) per side, ranging from the root to the empennage tip. Each pad had two hydraulic actuators connected at its ends, enabling combinations of shear and torque to be applied on each load station. Figure 2 presents a sketch of test setup.

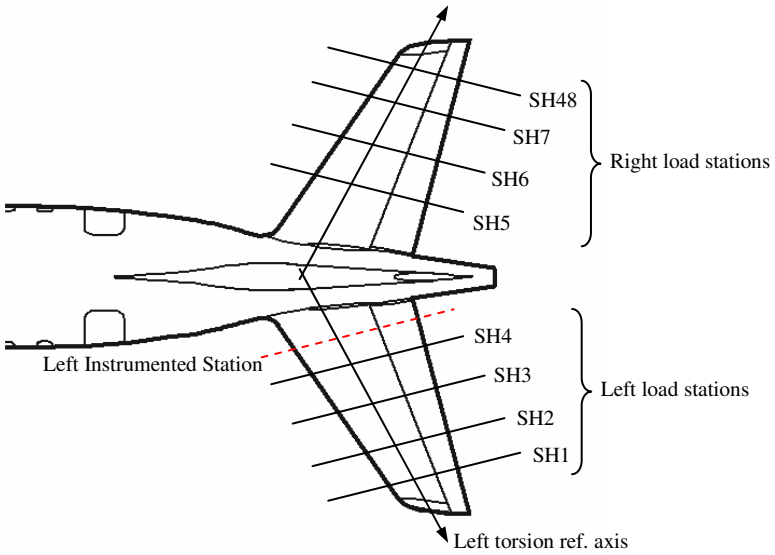

Figure 2: General test setup

The calibration loads were successively applied on each load station and also on each pair of symmetrical load stations individually, providing the experimental data for the calibration.

Moreover, a distributed load representing one flight condition was also applied over all load stations simultaneously through a whiffletree scheme. This latter load condition, which was intended to simulate a distributed load corresponding to a pull-up maneuver, was not used as input to generate the calibration results, but instead, it was used to demonstrate the applicability and reliability of the load equations to reproduce a generic applied load closer to the real condition.

Among the available bridges, the calibration was conducted for the left side instrumentation using responses of 2 bending bridges (A20638 and A20639), 2 shear bridges (A426 and A429), and 3 torque bridges (A430 and A431), along with the applied calibration loads.

According to the regression analysis presented by Skopinski et al (1954), load equations were fitted to the experimental data so the loads could be determined through a linear function of the bridges responses. For the normal force (F), bending moment (M) and torque (T) actuating on the empennage, such relation is represented generically as follows:

$$F = \beta_{11}\mu_1 + \beta_{12}\mu_2 + \beta_{13}\mu_3 + ... + \beta_{1j}\mu_j \quad (1)$$

$$M = \beta_{21}\mu_1 + \beta_{22}\mu_2 + \beta_{23}\mu_3 + ... + \beta_{2j}\mu_j \quad (2)$$

$$T = \beta_{31}\mu_1 + \beta_{32}\mu_2 + \beta_{33}\mu_3 + ... + \beta_{3j}\mu_j \quad (3)$$

where μ_j is the j strain gage bridge response and β_{ij} is the j established calibration coefficient for the force i.

3. HYBRID CALIBRATION

In their work, Jenkins et al (1977) reported that a relatively simple model was able to accurately predict the character of the response (strains) of a wing structure to load. However, the prediction of the response's magnitude was less reliable. In general, a more accurate model would lead to a better response prediction, but still with discrepancies. In the present investigation, the model bridges were satisfactorily fitted to the actual bridges through a sample of experimental data, enabling the use of the predicted bridge responses into a load calibration.

3.1. Structural Model

The structural elastic model was built using NASTRAN 2D shell elements for the skin, ribs, spar webs and frame webs, and NASTRAN beam element for the stringers, spar flanges and frame flanges. Rigid elements were used to transfer the forces to the ribs, in order to reproduce the actual calibration tests. The rear fuselage boundary nodes 6 degrees-of-freedom were constricted. Figure 3 shows the structure mesh.

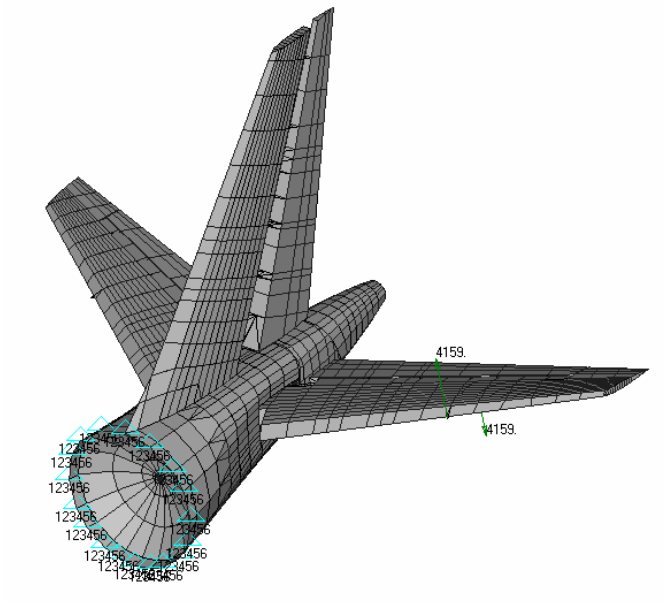

Figure 3: Finite element elastic model

3.2. Simulated Strain Gage Responses

The spar and skin elements (shell elements) on the model which were nearest to the strain gages on the real structure were selected for the analysis.

The structural model outputs the strains at discrete points. For the shell elements, the normal (ε_x and ε_y) and shear (γ_{xy}) strains are supplied on its corners and center. Thus, the strain gage bridge responses were built up by a proper manipulation of these discrete strains, pursuing the actual condition presented in Fig. 1. Taking as reference Fig. 4, which depicts the plane stress stated on a particular point of the shell element (corners or center), the x axis represents the spar direction for the spar elements or the torsion reference axis (see Fig. 2) direction for the skin elements. The y axis corresponds to the transverse direction on the element plane.

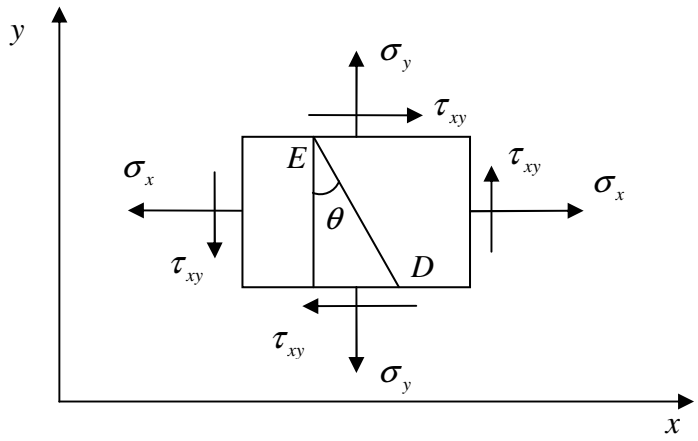

Figure 4: Stress state for a particular point

For applications involving small strains, the four-active-arms bridge response in terms of the individual arm strains (see Fig. 1) corresponds to:

$$\varepsilon_{bridge} = \varepsilon_1 - \varepsilon_2 + \varepsilon_3 - \varepsilon_4 \tag{4}$$

Based on the foregoing, the model bridges were simulated, as depicted next.

Shear and torsion bridges simulation: the strains at the element center were used as reference. Considering the actual installation, the shear and torsion bridge arms are rotated by 45° from the x direction. Thus, the strains at the element center were calculated for directions normal to the ED line in Fig. 4, considering $\theta = 45^\circ$ and $\theta = -45^\circ$. The normal strain for a direction perpendicular to the ED line ($\varepsilon_{n,\theta}$) is calculated as (Magson, 1990):

$$\varepsilon_{n,\theta} = \varepsilon_x \cos^2\theta + \varepsilon_y \sin^2\theta + \frac{\gamma_{xy}}{2}\sin 2\theta \tag{5}$$

And consequently the bridges may be simulated as follows:

$$\mu_{simulated\_shear\_bridge} = 2\varepsilon_{n,\theta=45^\circ} - 2\varepsilon_{n,\theta=-45^\circ} \tag{6}$$

$$\mu_{simulated\_torque\_bridge} = (\varepsilon_{n,\theta=45^\circ} - \varepsilon_{n,\theta=-45^\circ})_{upper\_skin} + (\varepsilon_{n,\theta=-45^\circ} - \varepsilon_{n,\theta=45^\circ})_{lower\_skin} \tag{7}$$

Bending bridges simulation: the strains at the element corners were used as reference (upper and lower inboard element grids), and the bridge may be simulated as follows:

$$\mu_{simulated\_bending\_bridge} = 2\varepsilon_{x,upper} - 2\varepsilon_{x,lower} \tag{8}$$

3.3. Model Loading

In order to submit the structural model to the same sort of loading used on the experiments, initially isolated unitary loads were applied to the model at the actuator application points and the response in terms of simulated bridges were tabled (4 load stations per side with two actuators each, requiring hence 16 unitary load cases).

Secondly, the bridge responses were compounded for the whole set of calibration loadings (as applied on the actual structure) according to the superposition principle applicable to the elastic linear model. Thus, considering a more general case where the calibration load is applied on a pair of symmetrical load stations (Fig. 5), a particular simulated bridge response is compounded as below:

$$\mu = \mu_{Act.1} * L_{Act.1} + \mu_{Act.2} * L_{Act.2} + \mu_{Act.3} * L_{Act.3} + \mu_{Act.4} * L_{Act.4} \tag{9}$$

where μ is the strain gage response due to the total loading, $\mu_{Act.n}$ is the response due to one unitary load at the actuator n application point, and $L_{Act.n}$ is the effective load applied by the actuator n. The Eq. (9) is dimensionally consistent since the term $\mu_{Act.n}$ is expressed in terms of microstrain per unit of load.

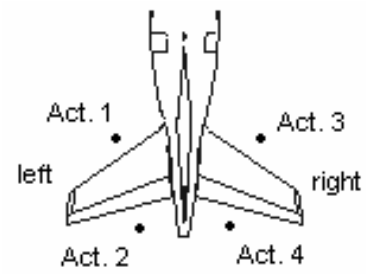

Figure 5: Symmetrical pair of load stations loaded

3.4. Adjustment of the Simulated Strain Gage Responses

Considering that the model exhibits a similar behavior but with distinct sensitivities from the corresponding physical structure, some adjustments based on the experimental data were needed. The perfect adjustment would result in a 1x1 correlation between the simulated and actual bridges responses for the whole set of applied calibration loads.

Based on a reduced set of experimental data corresponding to the SH3/SH6 loading cases, a satisfactory correlation was attained between the model and structure bridge responses for all applied calibration loads, except for the root load stations (SH4 and SH5). The methodology is developed next.

Through the analysis of the preliminary data with apparently no correlation among prototype and model responses, two distinct approaches,

- torque bridge alignment correction, and
- adjustment factors for different loading conditions (carry-over),

were elaborated, enabling the data transformation and the results presented here.

A particular bridge usually presents distinct sensitivities to torsion, bending and shear loading, and also to loads applied on the opposite side of the structure (carry-over effect), and so does its correspondent finite element from model.

The first adjustment was performed considering only the torsion bridges. In Fig. 6 (a), which presents the correlation between the model and structure response for the bridge A431, one can notice that different slopes take place, indicating distinct relations between the model and the experimental bridge responses to torque and bending.

The sensitivity of the torque bridges depends directly on its alignment on the member, according to the Eq. 7. So, the approach was to rotate the model element response a few degrees from its nominal position until the ratio between the model and the experimental strain gage bridge outputs was approximately constant for either bending and torsion loads.

Figure 6 (b) illustrates this procedure applied for the simulated bridge A431, considering the SH3 loading. A common slope is attained by a small rotation on the model bridge (4° from the original position). The same approach was performed for the other torque bridge (A430), and the rotation (from the original configuration) encountered was 2°.

The reason for the adjustment conducted above could be addressed to an eventual installation misalignment of the real parameter. Small strain gage installation misalignment might occur due to its reduced dimensions and installation conditions.

Once defined the rotation angle for the model torque bridges, the procedures to determine the adjustment factors for all bridges were carried out.

For the loading sequences applied at the left stations SH1, SH2 and SH3 (each one comprised by a shear force and a torque) the ratio between the model and the experimental output was found to be constant for each strain gage bridge. For the opposite side, loadings at stations SH6, SH7 and SH8, another constant ratio was found for each bridge.

Thus, in order to fit a particular bridge output from the model into the experimental value, two factors shall be used. The first one (C_1) shall be considered when the loading is applied at the same side of the instrumentation, and the second one (C_2) when it is on the opposite side (carry-over effect).

Such factors could be established considering the loadings at two symmetrical load stations, such as SH3 and SH6. The resulting adjustment factors would be valid for the other loadings (SH1/SH8 and SH2/SH7).

The adjustment factors (C_1 & C_2) change the Eq. 9 into

$$\mu_{adjusted} = (\mu_{Act.1} * L_{Act.1} + \mu_{Act.2} * L_{Act.2}) * C_1 + (\mu_{Act.3} * L_{Act.3} + \mu_{Act.4} * L_{Act.4}) * C_2 \quad (10)$$

for the left side instrumentation.

The sequence presented in Fig. 7 details how the adjustment factors C_1 and C_2 were used to fit the model into the experimental response for the torque bridge A431, after its alignment correction. In Fig 7(a), the model strain gage output (A431) was calculated from Eq. 9 (the adjustment coefficients were not applied yet and the alignment correction had been previously done). In Fig. 7(b) the coefficient C_1 is determined as $C_1 = 1/-0.8668 = -1.154$ (inverted fit line slope). In Fig. 7(c) the coefficient C_2 is determined as $C_2 = 1/-1.5764 = -0.634$ (inverted fit line slope). In Fig 7(d) the model response (A431) was adjusted through the factors presented above (using Eq. 10) in order to fit it into the experimental strain (the negative sign of coefficients changed the sign of the model bridge into the experimental bridge sign). It shall be realized that the factors C_1 and C_2, determined from the loadings at SH3 and SH6 load stations, were able to match the model and structure bridges for a set of loadings (SH1/SH8, SH3/SH6 and SH2/SH7).

The procedure as depicted in Fig. 7 was applied for the other model bridges.

After the manipulations presented in this section, the calibration coefficients were determined using as input the calibration loads at all load stations, and the corresponding model bridge outputs.

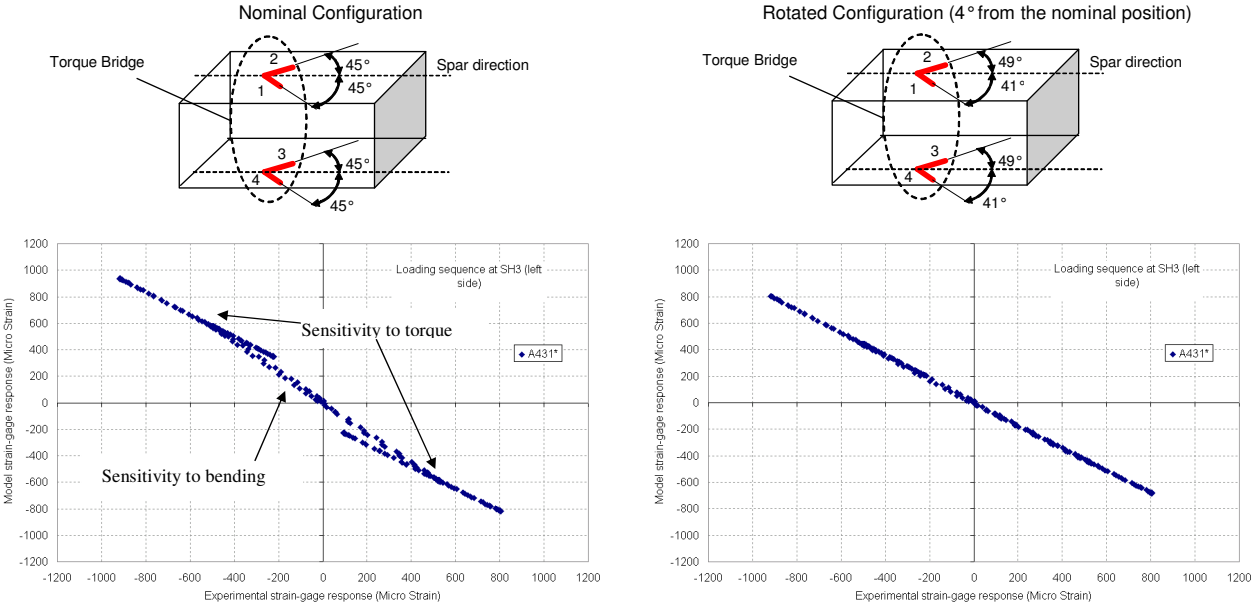

Figure 6: Model vs. experimental torque bridge responses for (a) nominal bridge positioning and (b) for a rotated configuration.

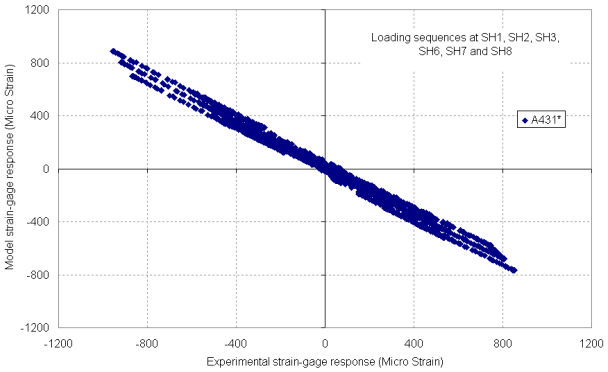

(a) Model vs. experimental bridge outputs for the load sequences applied at the SH1/SH8, SH2/SH7 and SH3/SH6 load stations

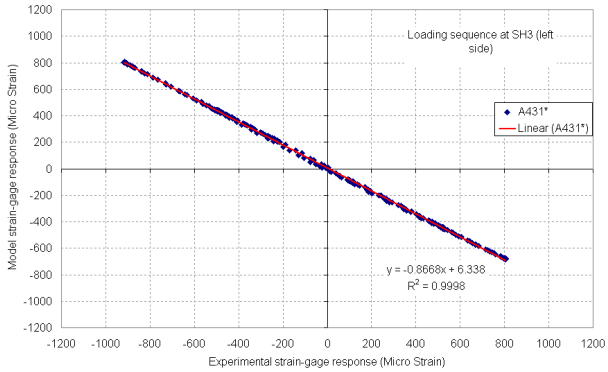

(b) Model vs. experimental bridge outputs for the loading sequence applied at the SH3 (same side of the instrumentation)

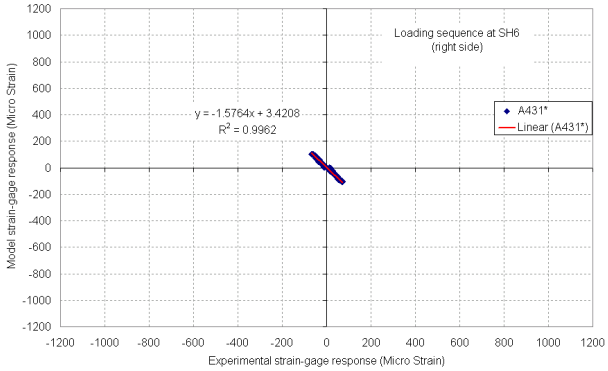

(c) Model vs. experimental bridge outputs for the loading sequence applied at the SH6 (opposite side to the instrumentation)

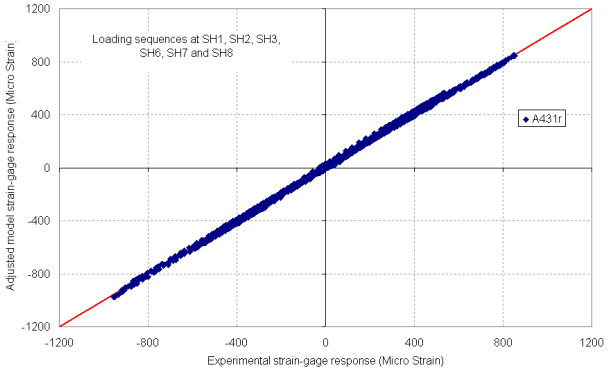

(d) Adjusted model vs. experimental bridge outputs for the loadings sequences applied at the SH1/SH8, SH2/SH7 and SH3/SH6 load stations

Figure 7: Sequence to adjust the model bridge into the experimental response

4. RESULTS

Similar to the conventional calibration, the load equations from the hybrid methodology were developed according to the regression analysis presented by Skopinski et al (1954), using the adjusted bridges responses calculated from the structural model and the corresponding loading conditions.

A set of calibration coefficients β were generated through the hybrid calibration, so the loads can be determined as shown in Eq. (1) to (3). The plots in Fig. 8 present for the considered loads (shear, bending moment and torque), the correlation between (a) applied ground load and calculated load from the hybrid calibration; (b) applied ground load and calculated load from the conventional calibration and (c) in-flight load calculated from the hybrid and conventional calibrations. The applied ground load comprises the loading sequences at the SH1, SH2, SH3, SH6, SH7, SH8 load stations and the distributed check loading, on which all the load stations were simultaneously loaded (SH1 to SH8). The left root instrumented station is referred to as 3H in Fig. 8.

The load measurement confidence intervals were established considering the spread of the calculated loads in relation to the applied loads (reference values). The criterion adopted corresponded to $\pm 3\sigma$, where 99.7% of the measurements lie within $\pm 3\sigma$ around the calculated load. The confidence intervals are indicated in Fig. 8 by the surrounding parallel lines in the plots (a) and (b).

Comparing the plots (a) and (b) in Fig. 8, one can notice that the conventional calibration is more accurate. This result was expected since the bridge response prediction from the hybrid calibration method is not exact.

The in-flight loads were determined for some flight tests using both calibration methodologies, and the results showed a good correlation, as shown in Fig. 8 (c). In order to have a comparison as general as possible, the loads were determined considering flight test data for a large range of flight parameters (alpha, beta, load factor, airspeed and Mach number).

One important advantage of the simplified calibration consists in using a reduced amount of experimental data to adjust the model, so that the actual strains can be satisfactorily predicted for different load application along the structure.

In the case of loading applied at the SH4/SH5 load stations, the strain prediction was less reliable. Consequently, the loads applied at SH4/SH5 were not well reproduced by using the load equations derived from the hybrid calibration. The load stations SH4/SH5 are closer to the instrumented station and the local effects may not be properly reproduced by the model.

But in the general the results were found to be acceptable, with a good agreement between the conventional and hydride calibrations results for most of the applied calibration loads and the distributed check loading, as presented in

Fig. 8. In addition, it was verified that the in-flight loads calculated from the hybrid calibration matched satisfactorily with those calculated from the conventional calibration (Fig. 8, plots (c)).

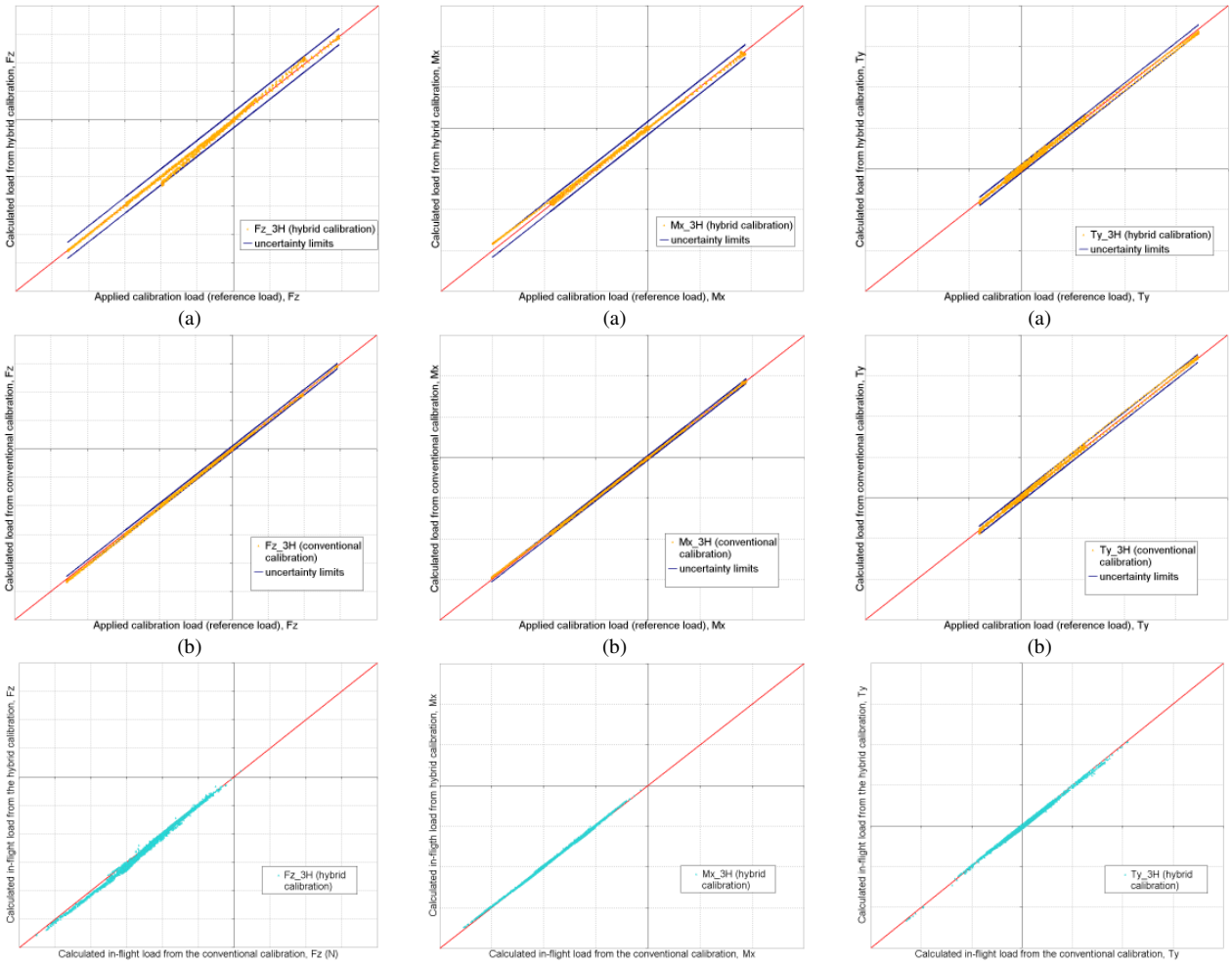

Figure 8: Correlation between the calculated and applied loads (shear, benging moment and torque) for (a) hybrid and (b) conventional calibrations; (c) correlation between the in-flight loads determined by the two calibrations.

5. CONCLUSIONS

For the structure investigated, the hybrid calibration method showed in general satisfactory results, indicating that the method could be extended for other conventional aeronautic surfaces which hold a similarity in terms of construction conceit.

Comparing with the conventional calibration, some advantages may be identified for the hybrid calibration methodology, as listed below:

a) Scope of the calibration tests restricted to the adjustment of the theoretical model, with the reduction of the calibration test cases;

b) Flexibility to consider several distinct calibration loading conditions through the model. This characteristic allows a complete set of calibration loading cases to be considered for the calibration coefficients determination, some of them difficult or costly to implement;

c) Possibility to verify the current calibration for several and different known distributed loading cases.

Despite the higher uncertainties related with the hybrid calibration, the general results derived from this alternative methodology are promising in the sense that it could be applicable for other practical situations. Other calibrations programs should be performed according to the conventional method and the hybrid calibration performed in parallel. Comparisons of the results will indicate the applicability and reliability of the new methodology for a more general situation. In doing so, the hybrid calibration could achieve the necessary level of maturity to be adopted instead of the conventional method.

6. BIBLIOGRAPHY

Jenkins, J.M. et al, 1977, "Strain Gage Calibration of a Complex Wing", J. Aircraft, Vol. 14, No. 12, pp. 1192-1195.
Magson, T.H.G., 1990, "Aircraft Structures for Engineering Students", Second Edition, Halsted Press, New York, USA, 21 p.
Skopinski T.H. et al, 1954, "Calibration of Strain gage Installations in Airplane Structures for Measurements of Flight Loads", Report 1178, USA: NACA.

7. RESPONSIBILITY NOTICE

The authors are the only responsible for the printed material included in this paper.